Journal of Photochemistry, *38* (1987) 217 - 238

SOLVENT EFFECTS ON THE FLUORESCENCE PROPERTIES OF ANILINES

GOTTFRIED KÖHLER

Institute for Theoretical Chemistry and Radiation Chemistry, University of Vienna, Währingerstrasse 38, A-1090 Vienna (Austria)

(Received July 29, 1986)

Summary

Fluorescence spectra, quantum yields and lifetimes are comparatively studied for aniline, *N*,*N*-dimethylaniline (DMA) and some further alkyl-substituted and rigid aniline derivatives in various solvents. A good correlation of Stokes shift with macroscopic solvent parameters is found for DMA but not for aniline. General and specific solvent effects are distinguished by studying the functional dependence of various spectroscopic and photophysical parameters on the polar co-solvent concentration in binary solvent mixtures. Excited state complexation of primary and secondary amines with alcohols is demonstrated by the double-exponential decay of the monomer fluorescence and the grow-in of exciplex emission found in aniline–ethanol–*n*-hexane ternary systems. Exciplex formation is attributed to solvent–donor hydrogen bonding and primarily causes enhanced intersystem crossing compared with that in the free molecule, an effect also evoked by *N*-methylation. Non-specific long-range interactions give rise to a general reduction in the non-radiative deactivation rate, with the exception of *o*,*o*′-dimethyl-substituted anilines, for which an increase in this rate was found as the bulk becomes polar.

1. Introduction

Solute–solvent interactions bring about considerable changes in spectroscopic as well as in photophysical properties such as spectral shifts, intensification of the emission and also fluorescence quenching in some specific solvents. Solvent-induced shifts of the absorption and emission spectra were extensively studied and provide a well-established probe of electronic redistribution, *i.e.* changes in the molecular dipole moment on excitation [1 - 3].

Solvent effects on fluorescence spectra were classified recently in terms of general and specific effects [4]. General effects are related to the electronic polarization, which is determined by the refractive index of the medium, and to the molecular polarization, determined by the static

0047-2670/87/$3.50

dielectric constant. As these properties differ for the ground and the various excited states, solute–solvent interactions cause solvent-induced changes in their energy separation, *e.g.* singlet–triplet splitting. Consequently, variations in the rates and yields of the various deactivation processes result [5]. Specific interactions, which comprise all these local interactions, such as hydrogen bonding, charge transfer, proton transfer etc., lead to an essential modification of the electronic structure and, therefore, to considerably stronger effects on spectra and photophysical parameters [5 - 7]. Many questions arising in the interpretation of solvent-induced changes in the various decay rates still remain open.

The fluorescence properties of some polar benzene derivatives such as phenols and anilines were shown to depend considerably on the molecular environment [8 - 10]. The fluorescence quantum yield q_f and lifetime τ_f of phenol, only small when dissolved in hydrocarbons, increase remarkably in polar, hydrogen-bonding solvents (alcohols, ether) [8, 9]. Isoelectronic aniline, however, exhibits an opposite solvent effect on the fluorescence efficiency as these quantities are largest in hydrocarbons and decrease with increasing polarity [10]. Furthermore, strong energy effects on q_f were observed in non-associating liquids and these effects were related to hydrogen-bond formation as well as to OH and NH bond splitting respectively [11 - 13]. Hydrogen-bond formation was shown previously to have important effects on fluorescence spectra of 1,2,3,4-tetrahydroquinoline (THQ) (Scheme 1) and the equilibrium constant for complex formation increases considerably when the molecule is excited [14]. Excited state complexation of some aliphatic amines (triethylamine) and of the highly polar aniline derivative *p*-cyano-*N*,*N*-dimethylaniline with alcohol molecules was demonstrated by time-resolved fluorescence spectroscopy [15 - 17]. Furthermore, a detailed study of the solvent-dependent photophysics of 1-aminonaphthalines was reported recently [18].

In the present study solvent effects on the fluorescence properties of aniline and some of its derivatives are reported. The purpose of the present work was to discuss effects of molecular environment on the spectra and the various decay processes in relation to the molecular structure. Furthermore, special attention was paid to differentiate between general and specific solute–solvent interactions and to discuss the structure of excited solute–solvent complexes.

2. Experimental details

Aniline, *N*-methylaniline (*N*-MA), *N*,*N*-dimethylaniline (DMA), THQ, 2,6-dimethylaniline (2,6-DMA) (all best available quality; Merck, Darmstadt) and julolidine (see Scheme 1) (Aldrich, Steinheim) were further purified by distillation in vacuum. 2,6-*N*,*N*-tetramethylaniline was synthesized using a standard method [19]. Purity was checked by gas chromatography (generally better than 99.9%; 2,6-*N*,*N*-tetramethylaniline better than

99.995%) and the compounds were kept under an argon atmosphere. All solvents were of the best available quality (at least for spectroscopic use), further purified by standard methods when necessary and stored under an argon atmosphere. *n*-Hexane was generally dried by column chromatography over silica gel (Woelm, activity I) and Al_2O_3 (Aluminia Woelm B, activity I) and ethanol by distillation and refluxing over 10 Å molecular sieves. Oxygen was removed by bubbling with pure argon or by freeze–pump–thaw cycles. The temperature was kept constant at 21 °C for all measurements.

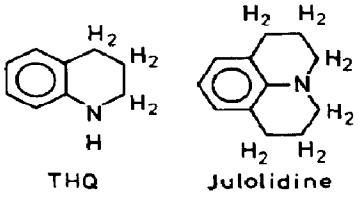

Scheme 1.

The fluorescence unit, connected with an Apple II microcomputer and a plotter on line, has been described previously (optics from Zeiss, F.R.G., monochromators M 4 QIII) [9]. Quantum yields were calculated by direct integration of the corrected spectra (quanta per unit wavenumber) according to the procedure given in ref. 13. The centre of gravity of the spectra, defined by

$$\langle\tilde{\nu}_f\rangle = \frac{\int f(\tilde{\nu})\tilde{\nu}\,d\tilde{\nu}}{\int f(\tilde{\nu})\,d\tilde{\nu}} \quad (1)$$

($f(\tilde{\nu})$ is the spectral distribution of the fluorescence light) and the half-bandwidth (HBW) were determined from the original data automatically.

Fluorescence decay profiles were obtained by time-correlated single-photon counting (Model SP 70, Applied Photophysics Ltd., London, slightly modified in our laboratory). The reconvolution of the data, collected by the Apple II microcomputer, was performed using a program based on a sum of exponential least-squares fit code by Kirkegaard [20] and origin shifts were considered automatically. Plots of weighted residuals and of the autocorrelation function, the value of reduced χ^2 and the mean errors were used to judge the quality of the fits [21]. A detailed description of the experimental procedure and the calculations, especially the consideration of energy effects on the instrumental response function, is given elsewhere [22].

3. Results and discussion

3.1. Absorption spectra and ground state associations

The near-UV absorption spectrum of aniline in hydrocarbon solution consists of two broad absorption bands peaking around 34.7×10^3 and 44.4×10^3 cm^{-1} and the first band shows some vibrational structure. In

alcoholic solutions broadening of the bands causes loss of structure and the transition moment decreases slightly. In hydroxylic solvents the spectrum shifts slightly to higher energies, whereas in ether solutions spectral shifts to lower energies are observed (Table 1). Nevertheless, solvent effects on the absorption spectra of anilines are generally small and have been studied in some detail previously [23, 24].

TABLE 1

Absorption maxima of some anilines in various solvents

Solvent	$\tilde{\nu}_a^{max}$ ($\times 10^3$ cm^{-1})					
	Aniline	*DMA*	*NMA*	*2,6-DMA*	*THQ*	*Julolidine*
n-Hexane	34.72	33.64	33.97	35.26	33.11	32.36
Ethanol	34.90	33.56	33.78	35.11	33.07	32.36
Tetrahydrofuran	34.25	33.43	—	—	—	—
Dioxane	34.54	33.41	—	—	—	—

In order to differentiate between local and long-range solvent effects the variation caused by the successive addition of alcohols to aniline solutions in *n*-hexane was followed. For 0.01 - 1.0 M ethanol the lowest band shows predominantly slight broadening. Following the procedure given in ref. 24 the equilibrium constant K for ground state associations, $K \approx 1.0$ M^{-1} ($T = 295$ K), was estimated from the rising absorptivity near the low energy onset of the band. This value agrees satisfactorily with data obtained by IR spectroscopy, since association constants for anilines with alcohols and ethers below or around unity have generally been reported [25, 26]. For DMA as proton acceptor in hydrogen bonds formed with methanol, a slightly larger value, $K = 1.7$ M^{-1} ($T = 20$ °C), was found recently [27]. The THQ–dioxane and THQ–ethanol systems were studied in more detail by UV absorption and fluorescence spectroscopy and the association constants $K = 3.72$ M^{-1} and $K = 4.00$ M^{-1} respectively were obtained [14, 24].

Anilines are thus only weak hydrogen-bonding agents and solvent shifts of absorption bands suggest that the bond is primarily formed between the hydrogen of the solvent and the nitrogen lone pair [23, 27]. This interaction is characterized by charge transfer from the nitrogen to the oxygen of the solvent, and a shift of the spectrum to higher energies results [25]. In cases where the amine is the proton donor, such as in THQ–dioxane, charge transfer is from the solvent to the amine and a shift to lower energies is observed. The K values indicate that ground state associations in binary solvent systems should become noticeable at alcohol or ether concentrations above 0.1 M.

3.2. Solvatochromic effects on the fluorescence

Large solvent-induced shifts are observed for the fluorescence spectra (maximum $\tilde{\nu}_f^{max}$) of anilines (Tables 2 and 3). Since absorption maxima

TABLE 2

Fluorescence data for 10^{-4} M aniline in various solvents (T = 22 °C)

Number	*Solvent*	$\tilde{\nu}_f^{max}$ ($\times 10^3$ cm^{-1})	$\langle\tilde{\nu}_f\rangle$ ($\times 10^3$ cm^{-1})	q_f	τ_f (ns)	k_F ($\times 10^7$ s^{-1})	k_{NR} ($\times 10^7$ s^{-1})
1	*n*-Hexane	31.73	31.11	0.17	4.42	3.8	18.0
2	Dioxane	30.34	29.81	0.16	3.60	4.4	23.0
3	Dibutyl ether	30.62	30.04	0.14	3.56	3.9	24.0
4	Diethyl ether	30.62	29.97	0.12	3.07	4.0	29.0
5	Butyl chloride	31.18	30.49	0.13	3.24	4.0	27.0
6	1,2-Dichloroethane	30.73	30.14		0.75		
7	Tetrahydrofuran	30.19	29.59	0.12	2.98	4.0	34.0
8	1-Butanol	29.65	29.15	0.12	3.00	4.0	29.0
9	2-Propanol	29.69	29.13	0.12	3.05	4.0	29.0
10	Ethanol	29.71	29.12	0.13	3.14	4.2	28.0
11	Methanol	29.75	29.12	0.12	2.91	4.1	30.0
12	Acetonitrile	30.34	29.72	0.15	3.50	4.3	24.0

TABLE 3

Fluorescence data of 10^{-4} M *N,N*-dimethylaniline in various solvents (T = 22 °C)

Number	*Solvent*	$\tilde{\nu}_f^{max}$ ($\times 10^3$ cm^{-1})	$\langle\tilde{\nu}_f\rangle$ ($\times 10^3$ cm^{-1})	q_f	τ_f (ns)	k_F ($\times 10^7$ s^{-1})	k_{NR} ($\times 10^7$ s^{-1})
1	*n*-Hexane	30.24	29.48	0.11	2.35	4.7	38.0
2	Dioxane	29.16	28.50	0.15	3.20	4.7	27.0
3	Dibutyl ether	29.86	29.14	0.12	2.60	4.6	34.0
4	Diethyl ether	29.46	28.92	0.11	2.25	4.9	39.0
5	Butyl chloride	29.36	28.68	0.13	2.61	5.0	33.0
6	1,2-Dichloroethane	28.86	28.30	0.028	0.90	(3.2)	108.0
7	Tetrahydrofuran	29.27	28.57	0.12	2.70	4.4	33.0
8	1-Butanol	29.16	28.35	0.12	2.74	4.4	32.0
9	2-Propanol	29.01	28.37	0.12	2.73	4.4	32.0
10	Ethanol	28.70	28.23	0.13	2.83	4.6	31.0
11	Methanol	28.39	28.12	0.13	3.01	4.3	29.0
12	Acetonitrile	28.46	27.97	0.17	3.80	4.5	22.0

($\tilde{\nu}_a^{max}$) are only slightly affected by the solvent, Stokes shifts, here defined by $\Delta\tilde{\nu}_s = \tilde{\nu}_a^{max} - \tilde{\nu}_f^{max}$, increase considerably when the polarity of the solvent increases. However, some caution is needed in interpreting variations in spectral maxima as Stokes shifts, as vibrational rearrangement in the excited state, by virtue of solute–solvent interactions, could significantly change the intensity distribution of fluorescence. Nevertheless, specific solvent interactions could become visible by such effects.

In correlating $\Delta\tilde{\nu}_s$ with solvent polarizability the expression recently given by Bilot and Kawski [28] was used:

$$\Delta\tilde{\nu}_s = \frac{(\mu_e - \mu_g)^2}{hca^3}\,\mathrm{BK} + \text{constant} \qquad (2)$$

with

$$\mathrm{BK} = \frac{\{(\epsilon - 1)/(2\epsilon + 1)\} - \{(n^2 - 1)/(2n^2 + 2)\}}{\{1 - \beta(n^2 - 1)/(2n^2 + 2)\}^2\{1 - \beta(\epsilon - 1)/(2\epsilon + 2)\}}$$

This approach correlates Stokes shift with the macroscopic solvent properties described by the refractive index n and the static dielectric constant ϵ. μ_g and μ_e are the dipole moments of the ground state and the excited state respectively, β is a factor taken as equal to unity, a the solute cavity radius, h Planck's constant and c the velocity of light. This equation assumes that the variation in Stokes shift with solvent polarity results from the change in the molecular dipole moment $\mu_e - \mu_g$ on excitation and that solvent effects are caused by long-range electrostatic interactions. This equation was shown recently to give the most reliable results in comparison with equivalent expressions [3] and provides a specific analysis of solvatochromic effects [29].

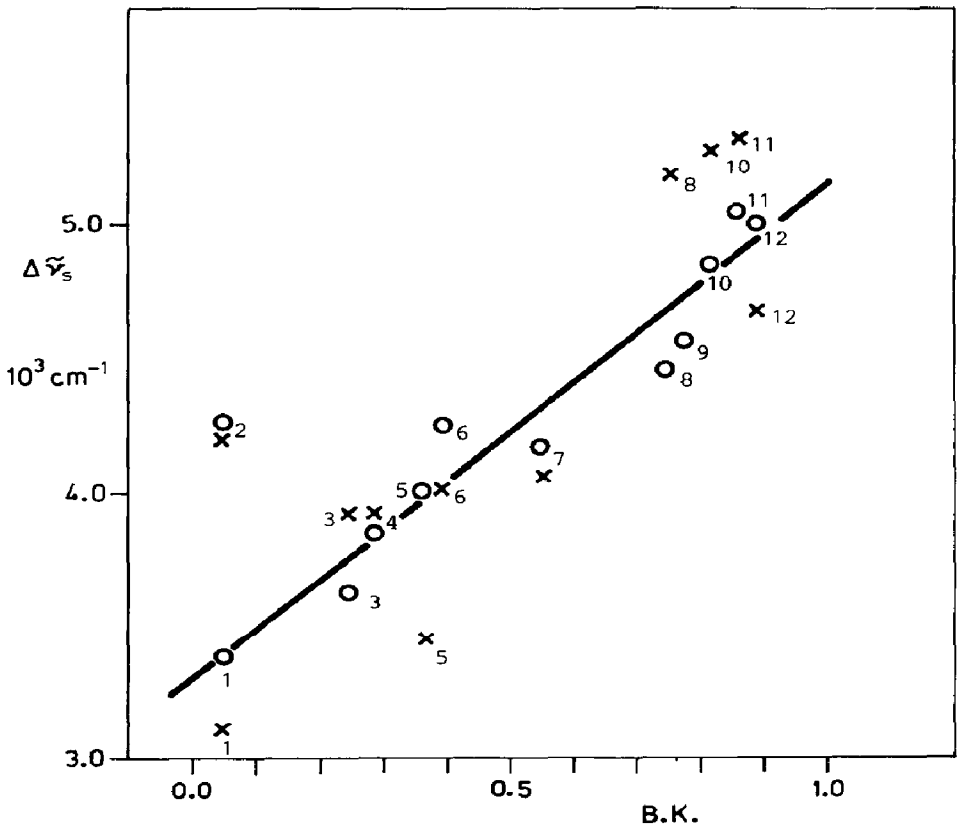

Fig. 1. Correlation of the Stokes shift $\Delta\tilde{\nu}_s$ (see text) of aniline and DMA with the BK values (see eqn. (2)) for various solvents (the numbers refer to the numbers of the solvents given in Table 2): ×, aniline; ○, DMA.

The Stokes shift $\Delta\tilde{\nu}_s$ obtained for aniline and DMA in 12 different solvents is plotted against the BK parameter in Fig. 1. For DMA, an excellent linear correlation according to eqn. (1) is obtained for all but one of the solvents considered. Excluding the exceptional case of dioxane from the regression analysis, an ascent of the regression line equal to 1830 ± 150 ($\Delta\tilde{\nu}_s$ is in reciprocal centimetres) was obtained. Assuming a solvent cavity radius of $a = 3.5$ Å an increase of 2.0 debye in the dipole moment $\Delta\mu$ results on excitation. However, $\Delta\mu$ depends critically on the assumed magnitude of a, which is subject to large uncertainties. $\Delta\mu = 0.85$ debyes was obtained recently by the Stark effect on the rotational fine structure of gas phase aniline [30]. In this respect, however, it was pointed out that the two methods for the determination of excited state dipole moments, *i.e.* solvent effects on the spectra and the Stark effect, measure different components of the dipole moment change and should thus give different results [31]. Nevertheless, $\Delta\mu$ for DMA is rather small, consistent with a small intramolecular charge transfer component of the lowest $\pi^* \leftarrow \pi$ ($1^1B_2 \leftarrow 1^1A_1$) transition, as discussed recently [31]. It is important that the Stokes shift of DMA correlates surprisingly well with the macroscopic solvent parameters.

Although $\Delta\tilde{\nu}_s$ for aniline follows in principle the same regression line, the deviation in the individual values is considerably larger than for DMA and no statistical significance for a linear correlation between $\Delta\tilde{\nu}_s$ and BK was thus obtained. Drawing a line through the values obtained in weakly associating solvents such as *n*-hexane, butyl chloride or acetonitrile, $\Delta\tilde{\nu}_s$ for dioxane solutions lies well off this line, nearly in quantitative agreement with the values for DMA. Furthermore, a consistent positive deviation is also observed for aniline in hydroxylic solvents.

The large deviation in aniline $\Delta\tilde{\nu}_s$ values imparts specific solute–solvent interactions in the excited state, which cannot be described by the polarization function BK and most likely arises from complexation reactions. This dissimilarity in the linear correlation between $\Delta\tilde{\nu}_s$ and BK for primary and tertiary amines is consonant with a recent study on solvatochromism of the 2-aminoanthracenes [29].

Most interestingly, aniline and DMA in dioxane solutions show an equal deviation in $\Delta\tilde{\nu}_s$. This suggests short-range interactions not primarily due to dioxane–proton donor hydrogen bonding [23, 24].

Specific local interactions should be apparent in spectral shifts and HBW data non-linearly related to the concentration of associating solvent in binary non-polar–polar solvent mixtures. Fluorescence spectra of aniline in some *n*-hexane–ethanol binary mixtures (Fig. 2) indicate complexation by the occurrence of a well-defined isoemissive point for ethanol concentrations less than 0.5 M.

Fluorescence maximum wavenumbers $\tilde{\nu}_f^{max}$ and the HBW of the spectra of some anilines in *n*-hexane solution are plotted *vs.* the concentration c_s of added ethanol or dioxane in Fig. 3. For all the primary and secondary amines considered (aniline, 2,6-DMA and THQ) $\tilde{\nu}_f^{max}$ decreases steeply at

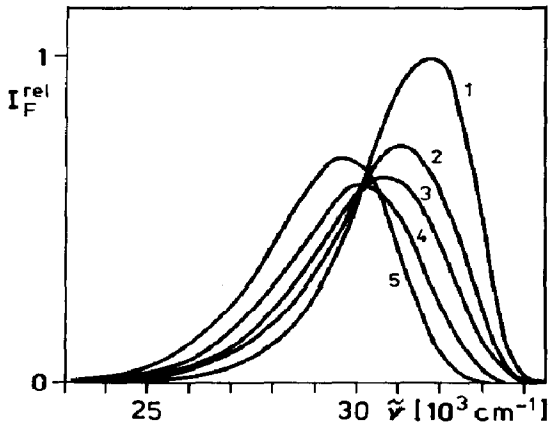

Fig. 2. Fluorescence spectra of 10^{-4} M aniline in various *n*-hexane–ethanol binary mixtures (excitation at 295 nm, T = 22 °C): curve 1, *n*-hexane; curve 2, 0.08 M ethanol; curve 3, 0.18 M ethanol; curve 4, 0.44 M ethanol; curve 5, pure ethanol.

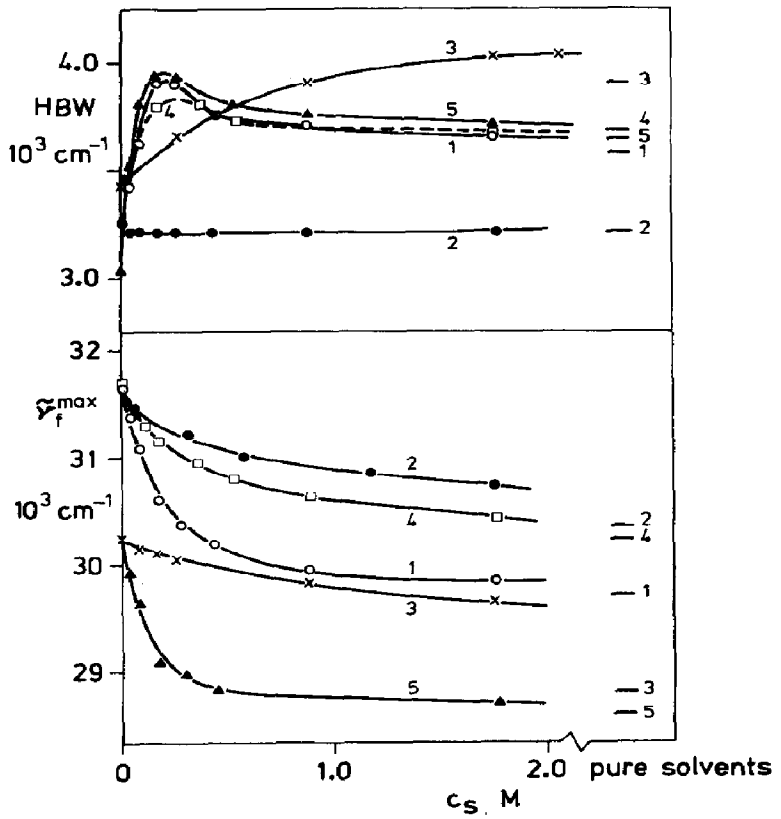

Fig. 3. A plot of the fluorescence maximum $\tilde{\nu}_f^{max}$ and the fluorescence HBW for various amines in *n*-hexane–ethanol or *n*-hexane–dioxane binary mixtures *vs.* the concentration of polar co-solvent: curve 1, aniline in *n*-hexane–ethanol; curve 2, aniline in *n*-hexane–dioxane; curve 3, DMA in *n*-hexane–ethanol; curve 4, 2,6-DMA in *n*-hexane–ethanol; curve 5, THQ in *n*-hexane–ethanol. The bars on the right-hand side give the respective values in the pure polar solvents.

$c_s < 0.2$ M but its variation becomes small when the alcohol concentrations exceed this value. The spectral shift in the DMA–ethanol and the aniline–dioxane systems varies nearly uniformly as the medium becomes polar.

The HBW increases when ethanol is added to *n*-hexane solutions of aniline, 2,6-DMA and THQ, goes through a maximum around 0.1 - 0.5 M ethanol and remains nearly independent of alcohol addition when $c_s > 1$ M. HBW data for DMA–ethanol likewise goes through a maximum value, but at a ten times larger ethanol concentration. In contrast, the HBW of aniline in the dioxane–*n*-hexane binary mixture remains constant when the solvent composition is varied and this system thus represents a notable exception.

The occurrence of maximum HBW in these ternary systems is related to the simultaneous existence of two distinct structures, the uncomplexed and complexed excited molecules. The spectra of both are strongly overlapping but slightly shifted in their maxima. Complexation might occur in the ground state causing insignificant changes in absorption spectra but larger effects on the emission, because of geometrical rearrangement in the excited state. They might, however, be formed following excitation as a consequence of altered properties in the excited state. A distinction between these possibilities might be obtained from a fluorescence kinetic study.

3.3. Solvent effects on fluorescence quantum yields and lifetimes

Fluorescence quantum yield and lifetime data are collected for aniline and DMA in various solvents and for some other aromatic amines in hexane and ethanolic solutions in Tables 2 - 4. q_f values for aniline, largest in hexane and decreasing in hydroxylic solvents, are in good agreement with some q_f data presented previously [10]. τ_f follows closely the same trend and this gives a radiative rate constant $k_F = q_f/\tau_f$ nearly independent of the solvent. Thus, the decrease in the fluorescence efficiency results predominantly from an increase in the non-radiative rate constant k_{NR} when *n*-hexane is replaced by associating or polar solvents.

The intersystem crossing rate k_{isc} was found to be larger in ethanolic than in cyclohexane solution and in the polar solvent both processes, fluorescence and triplet formation, account nearly quantitatively for the S_1 decay. In hydrocarbon solution a residual yield of about 10% remains for an unknown decay channel [10]. It might be interesting to compare aniline with isoelectronic phenol, for which a large deviation in $q_f + q_{isc}$ from unity was observed in hydrocarbon solvents [9]. This efficient non-radiative deactivation was associated with OH bond cleavage, a process quantitatively important for S_1 phenols [11]. No NH bond rupture was found for aniline when excited in its lowest state [12], consonant with $q_f + q_{isc}$ near to unity.

Qualitatively, the same solvent effects on q_f and τ_f, but larger in magnitude, are observed for 2,6-DMA (Table 4). Comparing 2,6-DMA with aniline, q_f and τ_f are higher in hexane solution but become nearly identical in ethanol. The non-radiative rate increases by a factor of 2 in the polar solvent compared with its value in hexane. A slightly larger k_F value agrees

TABLE 4

Fluorescence data of some substituted anilines in *n*-hexane and ethanol ($c = 10^{-4}$ M, $T = 22$ °C)

Substance	*Solvent*	$\tilde{\nu}_f^{max}$ ($\times 10^3$ cm^{-1})	$\langle\tilde{\nu}_f\rangle$ ($\times 10^3$ cm^{-1})	*HBW*	q_f	τ_f (ns)	k_F ($\times 10^7$ s^{-1})	k_{NR} ($\times 10^7$ s^{-1})
N-MA	*n*-Hexane	30.90	30.21	3.07	0.13	3.52	3.8	25.0
	Ethanol	29.16	28.62	4.62	0.14	3.88	3.6	22.0
2,6-DMA	*n*-Hexane	31.90	31.32	3.36	0.26	5.68	4.6	13.0
	Ethanol	30.29	29.86	4.82	0.15	2.93	5.3	29.0
THQ	*n*-Hexane	30.24	29.64	2.87	0.18	3.36	5.3	25.0
	Ethanol	28.56	28.04	4.51	0.19	3.57	5.4	23.0
Julolidine	*n*-Hexane	29.27	28.75	3.09	0.18	4.20	4.3	20.0
	Ethanol	28.13	27.80	4.23	0.15	3.62	4.2	23.0

with a general increase found for $S_1 \leftarrow S_0$ transition moments on *o*-methyl substitution [32].

Solvent effects on aniline decay processes can be summarized as follows: k_F depends insignificantly on the solvent, but k_{NR} increases in an associating and polar environment compared with its value in hydrocarbons. This rise in the efficiency of non-radiative deactivation can be attributed to enhanced singlet–triplet interconversion.

Solvent effects on DMA fluorescence are oppositely directed with respect to those on aniline fluorescence. The lowest quantum yield and lifetime is found in non-polar hydrocarbons whereas both values increase in a polar environment (Table 3). In alcohols, q_f and τ_f become nearly equal when comparing DMA with aniline. Since also for DMA, k_F remains nearly independent of solvent, the variation in the S_1 decay properties are attributed to a decrease in the non-radiative rate with rising solvent polarity.

Julolidine was considered in comparison with DMA: q_f and τ_f are larger for this compound and a considerably smaller non-radiative deactivation rate results. Ethanol causes a slight quenching of julolidine fluorescence, contrary to the enhancement of DMA fluorescence.

The dimethylamino group of julolidine is fixed coplanar to the aromatic ring and, most likely, in a pyramidal geometry. Aniline and DMA, both pyramidal in the ground state, are assumed to obtain a nearly planar configuration in the lowest excited singlet [31, 33 - 36]. In order to explain anomalies in the energy effects on the intersystem crossing rate of gas phase aniline the existence of a planar triplet $^3B_2$ was postulated recently at energies above the lowest non-planar $^3A_1$ [37]. Suppression of the non-radiative transitions in julolidine could thus be related to the non-flexibility of the molecule. Nevertheless, important effects of amino hydrogen motions and the geometry of the amino group on the S_1 deactivation rates are clearly

indicated by these results and supported by q_f and τ_f data of some other model anilines.

o-Methyl substitution should influence the non-radiative rate most importantly by steric hindrance of internal rotation about the Ar–N bond. In the case of DMA, one *o*-methyl group forces the dimethylamino group considerably out of the aryl plane [38] and thus affects electronic absorption spectra substantially [39]. Fluorescence of 2,6-*N*,*N*-tetramethylaniline was measured as an example of an aniline derivative exhibiting such large steric effects. In hydrocarbon solution, only weak ($q_f < 0.001$) emission around 345 nm (29 000 cm^{-1}) was observed with a short fluorescence lifetime ($\tau_f = 0.7 \pm 0.2$ ns) and in ethanolic solution no emission was found. Thus, out-of-plane rotation of the amino group strongly reduces the fluorescence efficiency and gives rise to large Stokes shift (absorption maximum at 266 nm). Such fluorescence quenching could probably be associated with internal charge transfer. In comparison, emission from an intramolecular charge transfer complex was reported for some tertiary phenylalkylamines [40].

Secondary amines such as *N*-MA and THQ (Table 3) show only a slight increase in q_f and τ_f when going from *n*-hexane to ethanol as solvent and k_{NR} is between the values for aniline and DMA. Furthermore, no significant difference in the fluorescence parameters is observed when comparing *N*-MA with THQ with an amino group fixed against rotation about the Ar–N bond. k_F is, however, exceptionally larger for THQ than for *N*-MA.

The fluorescence behaviour observed for the rigid aniline model compounds (julolidine, THQ and 2,6-*N*,*N*-tetramethylaniline) indicates that the phenyl ring and the amino group is indeed kept nearly coplanar in the excited state of anilines and out-of-plane rotation is not an important relaxational motion in excited state geometrical reorganization.

Temperature effects on q_f and τ_f of aniline and DMA in *n*-hexane and ethanol as solvents were measured in the range −15 to 55 °C and both values were constant within the error limits. This is consistent with earlier published data comparing fluorescence quantum yields of aniline in hydrocarbon and alcohol solutions at room temperature with those in glasses at 77 K. The non-radiative rate is, therefore, not enhanced as the temperature rises and the effect of local intermolecular interactions with ethanol molecules do not change significantly when the temperature is increased.

The lowest excited 1^1B_2 state is characterized by an increasingly polar structure, indicated by the larger dipole moment in the excited state. Excitation should thus stabilize intramolecular interactions, which are characterized by an increase in the charge on the nitrogen, and destabilize interactions causing transfer of charge in the opposite direction. From this it is concluded that hydrogen-bonded solvent–donor complexes should be stabilized in the excited state but bonding in solvent–acceptor complexes should become essentially weaker in the excited state. As ground state aniline acts predominantly as a proton acceptor, substantial geometrical

rearrangement of the local environment following excitation causes the marked solvent dependence of aniline fluorescence properties. This conclusion is consistent with the relatively small specific solvent effects on DMA emission, and a strengthening of THQ–dioxane and THQ–ethanol hydrogen bonds was indeed found recently [14].

3.4. Fluorescence of anilines in binary solvent mixtures

In pure polar solvents, effects of local interactions on excited state properties might be covered by long-range electrostatic interactions. In order to distinguish between these solvent effects, fluorescence quantum yields and lifetimes were studied in various binary solvent mixtures.

The q_f and τ_f of aniline decrease sharply when alcohol is added to the hexane to give a less than 0.5 M solution but increase slightly as the bulk becomes more polar (Fig. 4). Comparing these results with the spectral data shown in Fig. 3, the concentration ranges of maximum variation in photophysical properties and of largest relative spectral shift and maximum HBW correlate with each other. This proves aniline–alcohol complexation to be primarily effective on the non-radiative decay rates. However, the q_f and τ_f values of DMA increase gradually on ethanol addition and the variation in these quantities *vs.* $c_s > 4$ M is nearly identical for the two compounds. The slightly steeper q_f (τ_f) increase below 4 M ethanol might be due to weak local DMA–polar solvent interactions, consonant with the maximum HBW.

At ethanol concentrations $c_s > 2$ M, aniline fluorescence decay was successfully fitted to a single-exponential function, but below 1 M ethanol these fits had to be rejected. For example, the decay curves for *N*-methylaniline in *n*-hexane after the addition of ethanol to a concentration of

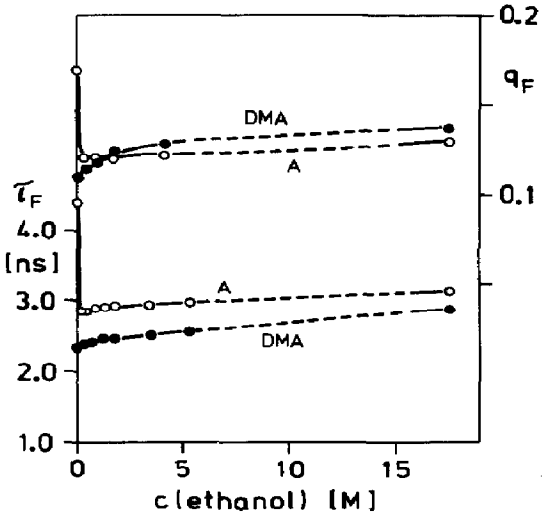

Fig. 4. Dependence of the fluorescence quantum yield q_f and the fluorescence lifetime τ_f of aniline and DMA on the ethanol concentration in binary ethanol–*n*-hexane solvent mixtures ($c = 1.10^{-4}$ M; $T = 21$ °C): ○, aniline; ●, DMA.

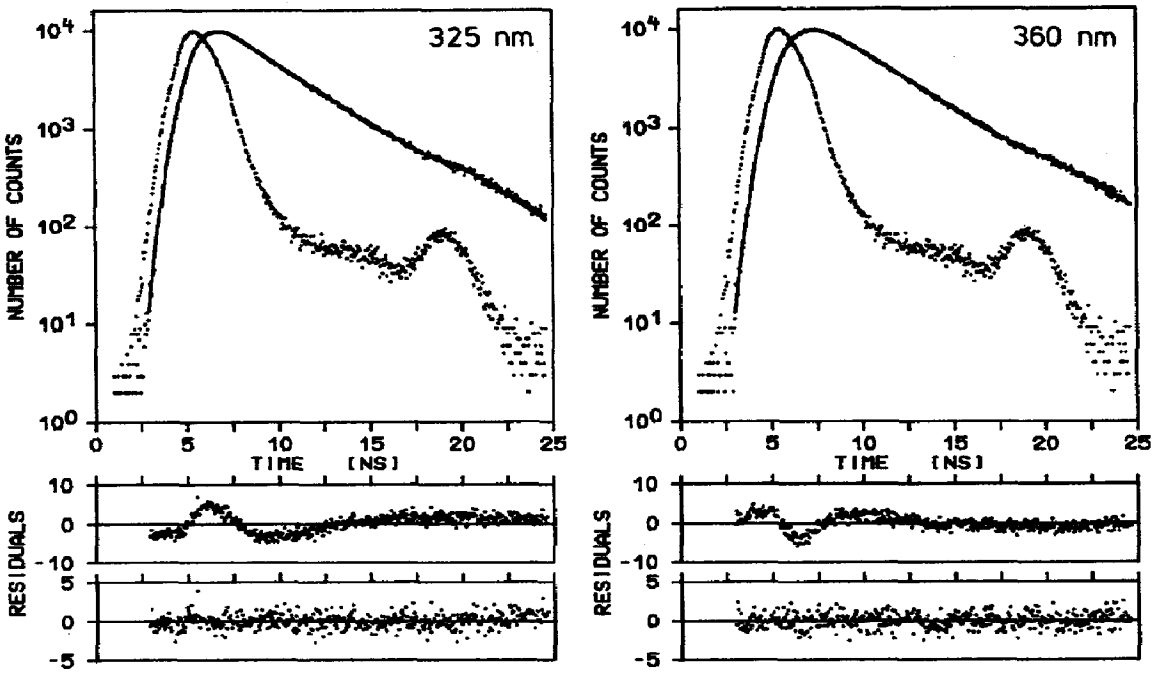

Fig. 5. Plots of fluorescence decay obtained for *N*-MA in *n*-hexane after addition of 0.21 M ethanol at an emission wavelength of 325 nm and 360 nm. The parameters obtained are collected in Table 5. The weighted residuals are plotted for a fit to a single-exponential function (upper plot) and to a sum of two exponentials (lower plot).

TABLE 5

Decay parameters resolved for some anilines in *n*-hexane solution after addition of ethanol at $T = 21$ °C (data for *N*-methylaniline correspond to decay curves given in Fig. 4)

Compound	*c*(ethanol) (M)	λ_{em} (nm)	τ_1 (ns)	a_1	τ_2 (ns)	a_2	χ^2
Aniline	0.18	310	3.22 ± 0.02	0.030	0.95 ± 0.05	0.015	1.03
		355	3.26 ± 0.02	0.043	0.85 ± 0.05	−0.018	1.04
N-MA	0.21	325	3.24 ± 0.01	0.034			5.46
			3.53 ± 0.01	0.027	0.69 ± 0.05	0.017	0.95
		360	3.63 ± 0.01	0.034			3.32
			3.52 ± 0.01	0.039	0.59 ± 0.05	−0.020	0.98
THQ	0.18	325	3.51 ± 0.02	0.023	0.75 ± 0.05	0.023	1.04
		365	3.50 ± 0.01	0.038	0.64 ± 0.05	−0.022	1.03
2,6-DMA	0.26	307	4.22 ± 0.02	0.030	1.07 ± 0.20	0.005	1.04
		342	4.17 ± 0.02	0.040	0.70 ± 0.20	−0.007	1.05

0.21 M and recorded at two emission energies, *i.e.* at a high energy corresponding to the emission range of free aniline (325 nm) and at the low energy flank of the spectrum (360 nm), are plotted in Fig. 5. The respective

plots of weighted residuals are shown for fits to a single-exponential decay function (upper plot) and to a sum of two exponential terms (lower plot). Trying only one exponential term gives non-randomly distributed residuals and a large χ^2 value for both emission wavelengths (Table 5). The fits improve when a sum of two exponentials is used and the χ^2 values become nearly unity. The parameters obtained for some anilines at representative alcohol concentrations are collected in Table 4. At the high emission energy a double-exponential decay and at the low energy a grow-in followed by a decay is indicated by the signs of the pre-exponential factors. This clearly demonstrates excited state complexation for the aniline–ethanol system. Contrary to aniline, no double-exponential decay was resolved for DMA in ethanol–hexane mixed solvents.

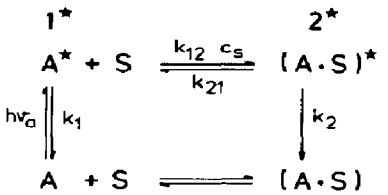

Scheme 2. (A ≡ aniline, S ≡ solvent.)

As fluorescence decay is clearly double exponential, excited state complexation can be treated like exciplex kinetics according to Scheme 2. The mathematical treatment leads to a system of two linear differential equations and the time dependence of monomer and complex fluorescence intensities, i_1 and i_2 respectively, are given by [21, 41]

$$i_1 = a_1 \exp\left(-\frac{t}{\tau_1}\right) + a_2 \exp\left(-\frac{t}{\tau_2}\right)$$
$$i_2 = a_3 \exp\left(-\frac{t}{\tau_1}\right) + a_4 \exp\left(-\frac{t}{\tau_2}\right) \qquad (3)$$

and herein

$$a_3 = -a_4 \qquad (4)$$

The measured lifetimes can then be calculated from

$$\frac{1}{\tau_{1,2}} = \frac{1}{2}\left[k_1 + k_{12}c_s + k_2 + k_{21} \mp \{(k_1 + k_{12}c_s - k_2 - k_{21})^2 + 4k_{12}c_s k_{21}\}^{1/2}\right] \qquad (5)$$

One of these times is interpreted as the relaxation time and the other as the fluorescence decay time of the equilibrated system. It should be mentioned that the equality (4) is found only when the fluorescence spectra of 1* and 2* do not overlap significantly. Alternately, the fast decay of 1* and 2* cancel each other, at least in part.

Assuming formation of weak complexes, *i.e.* the dissociation rate is high ($k_{21} \gg k_1, k_2$), the relaxation time becomes

$$\frac{1}{\tau_R} \approx k_{12}c_s + k_{21} \tag{6}$$

For the equilibrium lifetime τ_E, which lies between $1/k_1$ and $1/k_2$ depending on the "equilibrium constant" K^*, one obtains under the same constraints the following equation:

$$\frac{1}{\tau_E} = \frac{k_1 + k_2K^*c_s}{K^*c_s + 1} \tag{7}$$

K^* can be defined by the ratio of the concentrations of 2^* to 1^* in equilibrium and this leads to the following expression:

$$K^* = \frac{[2^*]}{[1^*]c_s} = \frac{k_{12}}{k_2 + k_{21}} \tag{8}$$

and K^* becomes, assuming $k_{21} \gg k_1, k_2$, equal to the ratio of the rate constants for the forward and back reactions.

From steady state conditions the quantum yields of fluorescence from 1^* and 2^* become respectively

$$q_f^1 = \frac{k_F^1}{k_1 + k_2K^*c_s} \tag{9a}$$

$$q_f^2 = \frac{k_F^2K^*c_s}{k_1 + k_2K^*c_s} \tag{9b}$$

(k_F^1 and k_F^2 are the respective radiative rate constants for 1^* and 2^*).

The alcohol concentration dependence of the lifetimes and of the total quantum yield is plotted for aniline–ethanol in Fig. 6. The full lines drawn represent the concentration dependence of the data calculated using eqns. (5) and (9) and a set of best-fit rate constants collected in Table 6. Fractional yields q_f^1 and q_f^2 are given as broken lines. It is seen that the maximum in the HBW (Fig. 2) corresponds indeed to the concentration for which emission from complexed and uncomplexed forms has nearly equal weight.

The association reaction is nearly diffusion controlled (about 10^{10} s^{-1} in *n*-hexane) and the equilibrium constant, $K^* = 9.5$ M^{-1}, is approximately ten times larger than in the ground state. Replacing hexane by ethanol as solvent, k_F^2 does not vary within the limits of error. Refractive index effects on the radiative rate constant should be small as the refractive indices of these solvents are nearly identical [42]. Therefore, complexation affects mainly the non-radiative deactivation rate which decreases from $k_{NR} = 18 \times 10^7$ s^{-1} for free aniline to 36×10^7 s^{-1} for amiline–ethanol complexes, both in *n*-hexane solution. This latter value is near to k_{NR} of DMA in hexane (Table 3). As intersystem crossing accounts for at least 80% of the non-radiative deactivation of aniline in hexane, its rate should nearly double on complexation.

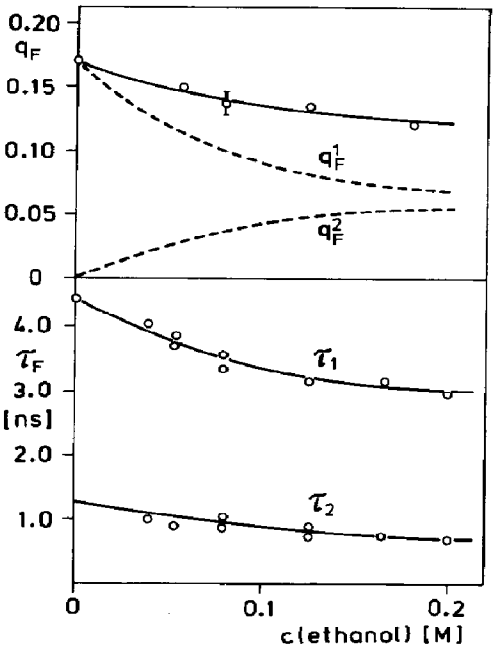

Fig. 6. Dependence of the fluorescence quantum yield q_f and the lifetimes τ_1 and τ_2 for aniline in the ethanol–*n*-hexane binary system on the alcohol concentration (T = 22 °C). The lines drawn through the data and the broken lines for the yields q_f^1 and q_f^2 (see text) were obtained from a 1:1 exciplex model using the parameters compiled in Table 6.

TABLE 6

Rate constants obtained for a best fit of the exciplex model (Scheme 2) to the obtained decay parameters for the aniline–ethanol and *N*-methylaniline–ethanol systems (see text)

Rate constant	*Aniline*	*N-MA*
k_1 (s^{-1})	2.22×10^8	2.84×10^8
k_2 (s^{-1})	4.0×10^8	2.8×10^8
k_{12} (M^{-1} s^{-1})	3.8×10^9	4.0×10^9
k_{21} (s^{-1})	4.0×10^8	3.2×10^8
k_F^1 (s^{-1})	3.77×10^7	3.8×10^7
k_F^2 (s^{-1})	4.1×10^7	3.8×10^7

The above-given considerations assume the formation of 1:1 excited state complexes and give a satisfactory explanation for the measured data. It should, however, be mentioned that in hydrocarbon solutions of alcohols, self-association was demonstrated at concentrations above 0.1 M [43]. However, neither the influence of a relative reduction in monomer concentration nor of the primarily formed tetramers was found and this might be due to the limits of error within which the parameters can be adjusted.

Increasing the polarity of the bulk suppresses non-radiative deactivation slightly: k_{NR} decreases from 36×10^7 to 28×10^7 s^{-1} for aniline–ethanol

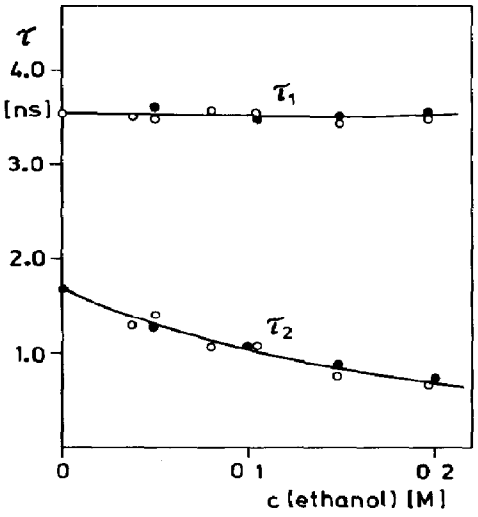

Fig. 7. Dependence of the fluorescence lifetimes τ_1 and τ_2 for *N*-MA in the ethanol–*n*-hexane (○) and the ethanol-d_1–*n*-hexane (●) binary system on the alcohol concentration (T = 22 °C). The lines are drawn for a 1:1 exciplex model using the parameters given in Table 6.

complexes and from 38×10^7 to 31×10^7 s^{-1} for DMA when the ethanol concentration is raised above 1 M. Thus, long-range interactions influence non-radiative deactivation of aniline oppositely to complexation reactions and the increase in k_{NR} in alcoholic solution is primarily due to the formation of hydrogen-bonded exciplexes. Long-range solvent effects are nearly identical in magnitude for aniline and DMA.

Also for 2,6-DMA, complexation is clearly indicated by the large effect of the alcohol concentration, $c_s < 0.5$ M, on q_f and τ_f in *n*-hexane–ethanol binary solvent mixtures (Fig. 7). Complexation causes qualitatively the same effects as for aniline. However, the non-radiative deactivation rate continues to increase as the polarity of the bulk rises. Therefore, long-range interactions seem to influence 2,6-DMA deactivation oppositely to that of aniline.

Although double-exponential decay is observed at some small ethanol concentrations in binary solvent mixtures, contributions of the fast component are only small (Table 5). τ_R is, however, of the same order of magnitude as for aniline. Therefore, it is concluded that complexation effects arise in this case predominantly from ground state associations, and excited state reactions are of comparatively minor importance.

Steric crowding by the *o*-methyl groups most probably causes a diminution of the dimerization rate, and excited state reactions become indistinguishable from ground state complexation. Reorganization of pre-formed complexes is fast and is, therefore, not resolved by the experimental set-up used. Bulk effects, opposite to those for aniline fluorescence, can be compared with those observed for julolidine fluorescence (Table 4). Also in

this case, an increase in the deactivation rate is found in the polar environment and this might result from electronic effects of *o*,*o*'-dimethyl substitution on the deactivation mechanism. Also for THQ, long-range effects on the lifetime are only small.

For the secondary amines, *N*-MA and THQ, excited state complexation is shown by the clear double-exponential decay observed in the ethanol–*n*-hexane mixed solvents (Table 5). The concentration dependence of the decay times and the grow-in time recovered by the fit procedure is plotted in Fig. 8 for the *N*-MA–ethanol system. Some best-fit parameters are compiled in Table 6. Most interestingly, no evident difference is observed when adding ethanol or deuterated ethanol. Although isotope exchange between the alcohol and the amine makes interpretation difficult, a deuterium isotope effect on the excited state association of anilines with ethanol is small and this supports the conclusion drawn above that the amines are proton donors in the excited state.

The deactivation rate of *N*-MA remains essentially constant on complexation (Table 6). k_2 decreases due to long-range bulk interactions. The variation is, however, only small when compared with that for aniline or for DMA. THQ behaves nearly identically with *N*-MA, but k_{NR} decreases slightly on complexation. Thus, restriction of intramolecular rotational motion has a small influence on the non-radiative deactivation of the molecule and primarily enhances the radiative transition rate. In total, solute–solvent complexation as well as long-range interactions affect k_2 of the

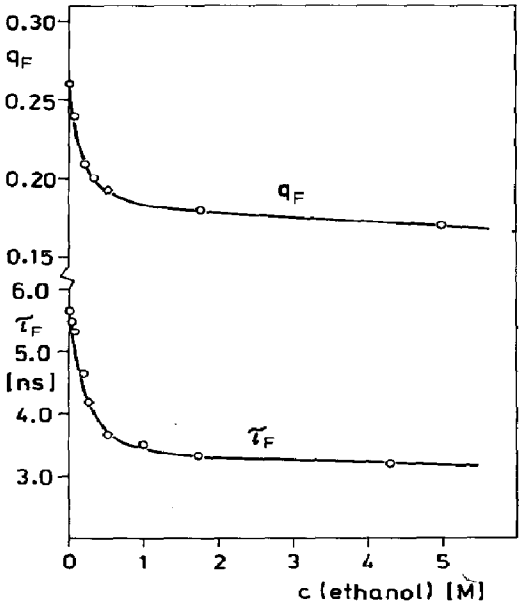

Fig. 8. Dependence of the fluorescence quantum yield q_f and the lifetime τ_f obtained for a fit of the decay to a single-exponential function for 2,6-DMA in the ethanol–*n*-hexane binary solvent mixture on the alcohol concentration (T = 21 °C).

secondary amines considerably less in comparison with that of the primary amines, aniline and 2,6-DMA.

The efficiency of S_1 non-radiative deactivation in these aniline analogues, smallest in the primary amines, increases essentially by both *N*-methylation and complexation by hydrogen bonding. Hydrogen bonding, with the amine as the proton donor, causes an increase in the negative charge on the nitrogen and thus a decrease in the effective ionization potential of the amino group which parallels the effect of *N*-methylation [31]. For both, a slight increase in the intramolecular charge transfer component is therefore expected, consonant with the effects on absorption spectra [31]. The lowest $^3A_1$ state was postulated to be non-planar [37] and thus is less sensitive to changes in the effective ionization potential of the amino group than the lowest planar $^1B_2$ singlet. Hence, singlet–triplet splitting should decrease on *N*-methylation and hydrogen bonding, and this would account for the increase in the intersystem crossing rate. No triplet should, however, lie near above the lowest singlet as q_f and τ_f are independent of temperature.

Also ethers as co-solvents could give rise to excited state complexation as they are effective proton acceptors. Furthermore, solutions in dioxane deviate considerably from the linear Bilot–Kawsky plot indicating local interactions as the reason for a larger spectral shift as calculated from an electrostatic model. However, the constant HBW of aniline in *n*-hexane–dioxane binary mixtures gives no hint of the appearance of two distinct and overlapping spectra.

The q_f of aniline decreases only slightly as the dioxane concentration is changed and its variation is near to the error limits of measurement. The quantum yield of DMA increases gradually as *c*(dioxane) rises. For both compounds the decay was clearly monoexponential at all dioxane concentrations tried. The monoexponential lifetimes *vs.* *c*(dioxane) are

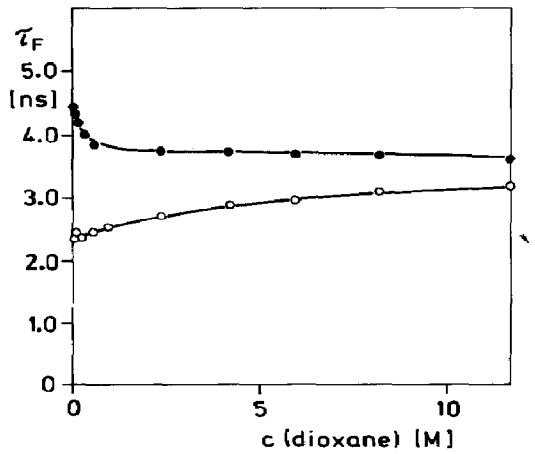

Fig. 9. Dependence of the fluorescence lifetime of aniline (●) and DMA (○) on the dioxane concentration in *n*-hexane–dioxane binary mixtures (T = 21 °C).

plotted in Fig. 9. Whereas τ_f for DMA increases parallel to q_f (k_F remains constant but k_{NR} decreases), τ_f for aniline drops significantly at concentrations below 1 M dioxane and only moderately above this concentration. Most of the increase in both rate constants, k_F and k_{NR}, of aniline thus occurs at low ether concentrations.

The observation of a single decay time does not, however, contradict *a priori* the occurrence of complexation reactions. A large dissociation rate k_{21} could probably make relaxation too fast to be resolved (see eqn. (6)). The concentration dependence of the lifetime would then be given by eqn. (7). Furthermore, ground state complexation could occur as well, although it can hardly be demonstrated because of the small effects on aniline absorption. Geometrical relaxation of such associates would be fast as no diffusional reaction is involved. Nevertheless, aniline–dioxane complexation by hydrogen bonding causes only small effects on the fluorescence spectra as (a) the shift of aniline fluorescence is not essentially more pronounced at low dioxane concentrations, (b) the HBW remains constant, and (c) spectral shifts are essentially equal for aniline and DMA. The formation of weakly bound excited aniline–dioxane complexes thus enhances the deactivation rate but the unusually large spectral shifts arise predominantly from specific interactions between the amine with high concentrations of dioxane in the bulk of the solution, different from hydrogen bonding.

4. Conclusions

The solvent dependence of Stokes shift of anilines results predominantly from shifts of the fluorescence spectra. For DMA the shift correlates sufficiently well with electrostatic parameters, except in the case of dioxane. Small contributions of specific solute–solvent interactions for the DMA–ethanol systems is consonant with the assumption that hydrogen bonds in which aniline is the proton acceptor are weakened in the excited state because of the smaller electron donor efficiency.

Fluorescence of primary and secondary aromatic amines (aniline, 2,6-DMA, *N*-MA, THQ) is primarily influenced by specific solute–solvent interactions. Formation of approximately 1:1 excited complexes with ethanol is clearly shown by excited state association kinetics, observed when alcohol is added successively to hydrocarbon solutions. Hydrogen bonds, with aniline as the proton donor, become stronger in the excited state by virtue of the increased charge acceptor strength. Such complexation causes primarily enhanced radiationless transitions for aniline and 2,6-DMA. No noticeable effects were found on the decay and the quantum yield of the secondary amines, *N*-MA and THQ. Both hydrogen bonding and *N*-methylation are expected to cause a decrease in singlet–triplet splitting and hence an increase in the intersystem crossing rate.

Complexation was also observed between aniline and dioxane, but not between DMA and dioxane. Exciplex formation by hydrogen bonding

does not, however, account for the exceptionally large spectral shifts observed in dioxane solution.

Non-specific long-range electrostatic interactions generally lead to a slight reduction in non-radiative deactivation; *o,o'*-dimethyl-substituted anilines represent an exception as k_{NR} increases in this case. The non-radiative deactivation of anilines is not temperature dependent.

Acknowledgments

The permanent help and encouragement by Prof. N. Getoff is gratefully acknowledged. I thank Mrs. K. Mayer for preparing the drawings and Dr. M. Gohn for the synthesis of some compounds. Financial support of the work by the Fonds zur Förderung der wissenschaftlichen Forschung (Project No. P4253) and by the Jubiläumsfonds der österreichischen Nationalbank (Project No. 2447) is appreciated.

References

1 W. Liptay, in E. C. Lim (ed.), *Excited States*, Vol. 1, Academic Press, New York, 1973, p. 129.
2 M. Nicol, *Appl. Spectrosc. Rev.*, *8* (1974) 183.
3 B. Koutek, *Collect. Czech. Chem. Commun.*, *43* (1978) 2368.
4 J. R. Lakowicz, *Principles of Fluorescence Spectroscopy*, Plenum, New York, 1983, Chapter 7.
5 J. B. Birks, *Photophysics of Aromatic Molecules*, Wiley Interscience, New York, 1970.
6 A. Weller, in G. Porter (ed.), *Progress of Reaction Kinetics*, Pergamon, London, 1961, p. 187.
7 R. B. Cundall and M. W. Jones, *Photochemistry*, Vol. 2, The Royal Society of Chemistry, London, 1981, p. 124.
8 G. Köhler and N. Getoff, *Chem. Phys. Lett.*, *26* (1974) 525.
9 G. Köhler, G. Kittel and N. Getoff, *J. Photochem.*, *18* (1982) 19.
10 G. Perichet, R. Chapelon and B. Pouyet, *J. Photochem.*, *13* (1980) 67.
11 G. Köhler and N. Getoff, *J. Chem. Soc., Faraday Trans. 1*, *72* (1976) 2101.
12 G. Köhler and N. Getoff, *J. Chem. Soc., Faraday Trans. 1*, *76* (1980) 1576.
13 J. Zechner, G. Köhler, G. Grabner and N. Getoff, *Can. J. Chem.*, *58* (1980) 2006. J. Zechner, G. Köhler, G. Grabner and N. Getoff, *Can. J. Chem.*, *59* (1981) 1744.
14 K. Chatterjee, S. Laha, S. Chakravorti, T. Ganguly and S. B. Banerjee, *Can. J. Chem.*, *62* (1984) 1369.
15 G. Köhler, *Chem. Phys. Lett.*, *126* (1986) 260.
16 Y. Wang and K. Eisenthal, *J. Chem. Phys.*, *77* (1982) 6076.
17 S. R. Meech and D. Phillips, *Chem. Phys. Lett.*, *116* (1985) 262.
18 S. R. Meech, D. V. O'Connor and D. Phillips, *J. Chem. Soc., Faraday Trans. 2*, *79* (1983) 1563.
19 W. L. Borkowski and E. C. Wagner, *J. Org. Chem.*, *17* (1952) 1128.
20 P. Kirkegaard, *Reports of the Danish Atomic Energy Commission*, Risø, Denmark, 1970.
21 D. V. O'Connor and D. Phillips, *Time-Correlated Single Photon Counting*, Academic Press, New York, 1984.

22 G. Köhler, *J. Photochem.*, *35* (1986) 189.
23 J. C. Dearden and W. F. Forbes, *Can. J. Chem.*, *38* (1960) 896.
24 T. Ganguly and S. B. Banerjee, *Can. J. Chem.*, *60* (1982) 741.
25 A. S. N. Murthy and C. N. R. Rao, *Appl. Spectrosc. Rev.*, *2* (1969) 69.
26 J. H. Lady and K. B. Whetsel, *J. Phys. Chem.*, *68* (1967) 1421.
27 T. Gramstad, *Acta Chem. Scand.*, *16* (1962) 807.
28 L. Bilot and A. Kawski, *Z. Naturforsch.*, *179* (1962) 621.
29 K. A. Abdullah and T. J. Kemp, *J. Photochem.*, *30* (1985) 363.
30 J. R. Lombardi, *J. Am. Chem. Soc.*, *92* (1970) 1831.
31 C. S. Seliskar, O. S. Khalil and S. P. McGlynn, in E. C. Lim (ed.), *Excited States*, Vol. 1, Academic Press, New York, 1974, pp. 233 - 242.
32 W. W. Simons (ed.), *The Sadtler Handbook of Ultraviolet Spectra*, Heyden, London, 1979.
33 M. H. Palmer, W. Moyes, M. Spiers and J. N. A. Ridyard, *J. Mol. Struct.*, *53* (1979) 235.
34 G. Barbieri, R. Benassi, R. Grandi, U. M. Pagnoni and F. Taddei, *J. Chem. Soc., Perkin Trans. 2*, (1979) 330.
35 J. C. D. Brand, D. R. Williams and T. J. Cook, *J. Mol. Spectrosc.*, *44* (1966) 359.
36 M. Quack and M. Stockburger, *J. Mol. Spectrosc.*, *43* (1972) 87.
37 R. Scheps, D. Florida and S. A. Rice, *J. Chem. Phys.*, *61* (1974) 1730.
38 J. P. Maier and D. W. Turner, *J. Chem. Soc., Faraday Trans. 2*, *69* (1973) 521.
39 H. B. Klevens and J. R. Platt, *J. Am. Chem. Soc.*, *71* (1949) 1714.
40 M. Van den Auweraer, A. Gilbert and F. C. DeSchryver, *J. Am. Chem. Soc.*, *102* (1980) 4007.
41 D. V. O'Connor and W. R. Ware, *J. Am. Chem. Soc.*, *98* (1976) 4708.
42 R. A. Lampert, S. R. Meech, J. Metcalfe, D. Phillips and A. Schaap, *Chem. Phys. Lett.*, *94* (1983) 137.
43 A. N. Fletcher, *J. Phys. Chem.*, *76* (1972) 2562.